

Artigo Original de Investigação

Identificação de lesões em esclerose múltipla: um método de segmentação em ressonância magnética

Identification of lesions in multiple sclerosis: a magnetic resonance imaging segmentation method

Inês Fernandes^{1*}, Ricardo Faustino²

¹ Faculdade de Ciências da Universidade de Lisboa, Departamento de Física, Lisboa. fc54895@alunos.ciencias.ulisboa.pt

² Escola Superior de Saúde da Cruz Vermelha Portuguesa, CrossI&D: Lisbon Research Center, Lisboa. rfaustino@esscvp.eu

A esclerose múltipla (EM) é uma doença imunomediada do sistema nervoso central que afeta o cérebro, a medula espinhal e os nervos óticos. A segmentação do cérebro por ressonância magnética (RM) é crucial para a avaliação diagnóstica, permitindo medir a extensão espacial das lesões e monitorizar o surgimento de novas lesões ao longo do tempo. A automatização da segmentação de lesões de EM de doentes em idade pediátrica, em imagens de RM, tem uma importância significativa para a prática clínica e a investigação biomédica, pois possibilita uma melhor caracterização dos achados imagiológicos, contribuindo para um diagnóstico mais preciso, um acompanhamento mais eficaz dos doentes e consequentemente um tratamento mais eficaz. Neste estudo exploratório, utilizámos um conjunto de imagens “*fluid-attenuated inversion recovery*” (FLAIR) de seis doentes diagnosticados com EM, adquiridas por um sistema de RM de 1.5T. A comparação estatística dos valores de intensidade dos pixels, realizada através do teste não-paramétrico de Wilcoxon, apresenta um valor de $p = 0,091$, não evidenciando diferenças estatisticamente significativas ($p > 0,05$) entre o método de limiarização e semi-automático. Contudo, o método semiautomático demonstrou potencial para uma maior precisão, especialmente na preservação de informação relevante. A reconstrução 3D revelou limitações, sugerindo a necessidade de futuras otimizações nos algoritmos de segmentação e na qualidade da reconstrução. Este estudo sublinha a importância do desenvolvimento de métodos automáticos mais robustos para aplicações clínicas e investigação em EM pediátrica.

Multiple sclerosis (MS) is an immune-mediated disease of the central nervous system that affects the brain, spinal cord, and optic nerves. Magnetic resonance imaging (MRI) segmentation is essential for diagnostic assessment, allowing for the detection and monitoring of lesion progression. This study proposes a semi-automatic segmentation method for FLAIR

images of paediatric MS patients, acquired using a 1.5T MRI system. Data from six patients were analysed using SPSS software to compare threshold-based and semi-automatic segmentation methods. The statistical comparison of pixel intensity values, performed using the non-parametric Wilcoxon signed-rank test, yielded a p-value of 0.091, indicating no statistically significant differences ($p > 0.05$) between the two methods. However, the semi-automatic method demonstrated greater potential for precision, particularly in preserving relevant information. The 3D reconstruction revealed some limitations, suggesting the need for further optimisation of segmentation algorithms and reconstruction quality. This study highlights the importance of developing more robust automated methods for clinical applications and research in paediatric MS.

PALAVRAS-CHAVE: Cérebro; esclerose múltipla; segmentação; reconstrução 3D.

KEY WORDS: Brain; multiple sclerosis; segmentation; 3D reconstruction.

Submetido em 12.09.2024; Aceite em 03.03.2025; Publicado em 31.03.2025.

* **Correspondência:** Inês Fernandes

Email: fc54895@alunos.ciencias.ulisboa.pt

INTRODUCTION

Multiple sclerosis

Multiple sclerosis (MS) is a chronic inflammatory and neurodegenerative disease of the central nervous system (CNS), which includes the brain, spinal cord, and optic nerves. In MS, the immune system attacks the myelin sheath—a protective layer that insulates neurons—leading to impaired or disrupted electrical signal transmission between nerve cells. This immune response results in the formation of inflammatory lesions in both grey and white matter, which can be detected using magnetic resonance imaging (MRI)¹.

In paediatric-onset MS (POMS), the disease typically exhibits a more pronounced inflammatory character compared to adult-onset MS (AOMS), often presenting with a higher number of lesions and greater disease activity in the early stages¹. Once the inflammation subsides, the damaged myelin areas may undergo a scarring process known as sclerosis.

Despite the aggressive inflammatory nature of paediatric MS, children tend to have a higher capacity for neural repair, including remyelination, which can delay the progression of disability. However, this repair potential does not preclude long-term risks, making early diagnosis and treatment crucial for managing disease progression effectively^{1,2}.

MS symptoms depend on multiple factors such as inflammatory reaction gravity, localization, and extent of lesions^{2,3}.

Based on the recent findings, the symptoms of multiple sclerosis (MS) vary in their onset, progression, and duration, depending on the clinical phenotype of the disease⁴. The classification of MS includes four primary clinical types, each defined by distinct patterns of disease progression and symptom presentation:

Relapsing-Remitting Multiple Sclerosis (RRMS): This is the most prevalent form of MS, characterized by clearly defined episodes of new or worsening

neurological symptoms, known as relapses or flare-ups. These episodes are followed by periods of remission, during which symptoms either stabilize, partially improve, or fully resolve. The duration of remission can range from several weeks to multiple years⁴.

Primary Progressive Multiple Sclerosis (PPMS): In this phenotype, the disease exhibits a continuous and gradual progression of neurological decline from the onset. Unlike RRMS, there are no distinct relapses, although temporary periods of stability or minor improvement may occur. This form of MS often leads to a steady accumulation of disability over time⁴.

Secondary Progressive Multiple Sclerosis (SPMS): Initially, individuals experience a relapsing-remitting course; however, over time, the disease transitions into a progressive phase marked by a gradual worsening of symptoms with or without intermittent relapses. This progression often signifies a shift from inflammatory activity to neurodegenerative processes⁴.

Progressive-Relapsing Multiple Sclerosis (PRMS): Although now considered a variant of PPMS in newer classifications, this form involves a steady progression of symptoms from the onset, combined with occasional relapses or exacerbations of more severe symptoms. It remains the rarest form of MS⁴.

Early symptoms:

During the initial stages of MS, common symptoms include blurred or double vision, muscle weakness, coordination difficulties, urinary incontinence, and dizziness. These symptoms often reflect the location and extent of demyelination within the central nervous system⁴.

Advanced stages:

As the disease progresses, patients may experience increased physical and mental fatigue, mood disturbances such as depression or anxiety, and cognitive impairments, including memory loss and difficulties with concentration. The severity and progression of these symptoms can vary significantly based on the type of MS and individual patient factors⁴.

Recent research suggests that transitions between phenotypes, particularly from RRMS to SPMS, are influenced by factors such as age at onset, relapse frequency, and MRI findings. Early identification and personalized treatment strategies remain essential to manage disease progression effectively and improve the quality of life for patients with MS⁴.

As of 2020, the Portuguese National Health Service (SNS) estimated a prevalence of over 8,000 MS patients in Portugal, while the World Health Organization (WHO) estimated a total prevalence of 2,500,000 MS patients worldwide⁵.

MRI in MS

MRI, introduced in the early 80's, revolutionized the study of MS by enabling *in vivo* observation of lesions' activity and effects⁶. Over time, the advancement of technology has made MRI an indispensable tool for visualising and analysing brain abnormalities in MS patients, supporting the diagnosis, monitoring, evaluation of therapeutic response and scientific research⁶.

It is common to distinguish advanced MRI (aMRI) from conventional MRI (cMRI). cMRI can be considered as a group of well-defined and highly standardized protocols, embodied in diagnostic criteria since the first guidelines of the International Panel⁷ Protocols and which include T2-weighted sequences, "fluid-attenuated inversion recovery" (FLAIR) sequences, "short-tau inversion recovery" (STIR) sequences and T1-weighted sequences before

and after gadolinium administration, in magnetic fields of 1.5T and above⁶.

Advanced imaging techniques such as Magnetization Transfer (MT), MR Spectroscopy (MRS), Diffusion-Weighted Imaging (DWI), and Susceptibility-Weighted Imaging (SWI) significantly improve the detection and characterization of MS lesions, especially at higher magnetic field strengths. MT imaging assesses interactions between free water protons and macromolecule-bound protons, offering valuable information on myelin integrity. The Magnetization Transfer Ratio (MTR), a key metric derived from MT, decreases with demyelination and axonal damage, making it a useful marker for disease progression and treatment response.

MR Spectroscopy (MRS) evaluates metabolic changes in brain tissue by measuring concentrations of compounds such as N-acetylaspartate (NAA), choline (Cho), and creatine (Cr). Reduced NAA levels often indicate neuronal damage, while elevated choline levels reflect increased membrane turnover associated with demyelination or gliosis. This technique helps in the early detection of neurodegeneration and distinguishes between active and chronic lesions.

Susceptibility-Weighted Imaging (SWI) is particularly sensitive to magnetic susceptibility differences, allowing the detection of iron deposition, microbleeds, and venous structures within MS lesions. It is especially effective in identifying the "central vein sign", a potential biomarker for MS diagnosis, and differentiates MS lesions from other white matter abnormalities. These advanced techniques contribute to earlier diagnosis, more accurate disease monitoring, and improved treatment strategies^{6,8}. Finally, the imaging protocol includes the administration of gadolinium, as a contrast agent⁶. Since the images used in this study

are FLAIR sequences, this technique will be further described.

Fluid-Attenuated Inversion Recovery (FLAIR) is an MRI sequence designed to suppress the signal from cerebrospinal fluid (CSF), effectively eliminating the hyperintense signal typically produced by CSF in conventional T2-weighted images. This suppression reduces the confounding effect of CSF on the visualization of lesions, particularly in periventricular and cortical regions, where MS lesions often occur. As a result, FLAIR enhances the contrast between MS lesions and surrounding brain tissue, allowing for clearer visualization and more accurate identification of lesion boundaries.

In addition to improving lesion detection, FLAIR provides detailed information about the localization, size, and morphology of lesions. It is especially effective in identifying juxtacortical, periventricular, and infratentorial lesions, which are characteristic of multiple sclerosis. While standard FLAIR imaging primarily aids in detecting chronic lesions, when combined with other MRI sequences or contrast-enhanced imaging, it can also help differentiate active (inflammatory) lesions from inactive ones by revealing new or enlarging lesions over time, which are indicative of disease activity⁹.

It may be important to use the FLAIR technique to address potential limitations such as detection of lesions in the posterior fossa and spinal cord¹⁰.

Segmentation

Brain segmentation refers to the process of separating different anatomical structures or regions-of-interest in brain images, in the MS context acquired through MRI.

Automated segmentation of MS lesions using MRI holds significant importance in clinical practice and research. Accurate segmentation of MS lesions is crucial for defining diagnostic criteria, such as the

spatial propagation of lesions (DIS) in MRI and the development of new lesions over time (DIT)^{11,12}. Additionally, automated segmentation allows quantitative analysis of the disease, enabling a better understanding of its progression and treatment options.

Traditionally, MS lesion segmentation relied on manual annotation by experienced neuroradiologists. However, this process is time-consuming and prone to significant variability among different observers. Therefore, developing automated methods for MS lesion segmentation is not only more efficient but also enables the calculation and interpretation of precise damage metrics, minimising the influence of subjectivity¹².

Although numerous automated methods for MS lesion segmentation have been reported in recent years, their adoption in clinical practice remains limited. A critical challenge is the overlapping intensity distribution between MS lesions and brain grey matter in MRI images¹³. This happens due to the limited image resolution, lesions' heterogeneity, and the complex shape of brain tissue, which affects many voxels located near the boundaries of different tissues¹⁴.

METHODOLOGY

Dataset

The dataset used in this study consists of a set of axial FLAIR MRI sequences of six patients diagnosed with MS, acquired with a Philips Achieva 1.5T MRI scanner with the following parameters: 8000 ms repetition time, 113 ms echo time, 150° flip angle; and a 208 x 230 mm² field-of-view. Of the six patients, four are male and two are female, with an average age of 16 years (Maximum age=19 years, minimum age=14 years, SD=1.75, IQR=3.5). All participants, along with their parents, provided informed consent to take part in this study, which

had prior approval from the local Ethics Committee at Centro Hospitalar e Universitário de Coimbra.

Prior to the analysis, the data set was converted from DICOM format to PNG format and subjected to a series of pre-processing steps. Firstly, the user selects a region-of-interest (ROI). The selected ROI surrounds the brain and is stored as a binary mask. This step, known as skull stripping or brain extraction, is a common pre-processing procedure. Subsequently, an attenuation factor of 0.1 is applied to the intensities of the image area outside the ROI. This step is necessary to reduce the influence of irrelevant structures, such as the skull.

Threshold-based segmentation

For the threshold-based segmentation of brain and lesion, the *Matlab* software and only the slices of each image sequence that had visible MS lesions were used.

As a first step, a histogram of the intensity map of the original image was generated. The histogram provides a visual representation of the frequencies of the different intensities present in the image. To determine the threshold value for segmenting the brain, a visual analysis of the histogram was adopted. This value was chosen manually as the minimum between two local maxima of the histogram. To obtain the best possible, adjustments were made to the threshold value interactively, which involved altering it up or down until the segmentation was as accurate as possible without losing information from the brain image. An example of a slice with an evident lesion and its respective histogram are displayed in Figure 1.

To segment the lesions, the same process was reproduced on the segmented image instead of the original image. The threshold values used for each slice are shown in Table 1. A curious relationship was observed where the values used for segmenting the

brain were approximately double those used for segmenting the lesions. Following this observation, the geometric mean of this relationship was calculated for further study.

The disadvantage of this process is that it is iterative and subjective, depending on the experience and skill of the person doing the segmentation. It is therefore important to evaluate results carefully and, if necessary, refine the segmentation based on additional criteria or more advanced methods.

Semi-automatic segmentation

For semi-automatic brain and lesion segmentation, the *Matlab* software was used once again.

On brain segmentation, first the code analyses the intensity distribution of each MRI brain image sequence by computing its histogram and the user selects two meaningful peaks. It then determines a threshold value based on the identified peaks. This threshold corresponds to the mean value of the bin with the lowest frequency, positioned between the selected peaks. By applying a mask with this threshold, we obtain the isolated brain. In some cases, an attenuation mask is needed to remove some noise from the image.

For lesion segmentation, the ratio identified between the two thresholds in the threshold-based segmentation method was applied. The same method was applied, but the threshold value for the lesion segmentation was multiplied by a factor of two times the threshold value for the brain segmentation. This adjustment maintains the initial ratio found between the two threshold values in the threshold-based segmentation, approximating unity. The resulting values are presented in Table 2.

3D reconstruction

To evaluate the 3D reconstruction of the brain, we employed the ImageJ software, which is a widely used open-source program for image analysis. We

utilized a series of brain segmentation images from a single patient. The segmentation threshold was established using the semi-automatic process detailed earlier, specifically focusing on the section where the lesion is most pronounced. This threshold value was then applied consistently across all slices in the sequence to ensure uniform segmentation. In ImageJ, we utilized the 3D Projection tool, incorporating interpolation between the slices and a spacing of 14 pixels to enhance the visual representation of the reconstructed brain volume.

Statistics

To examine potential discrepancies in pixel intensity values obtained through two distinct brain image analysis techniques, we conducted a Wilcoxon signed-rank test. This non-parametric statistical method was chosen due to its suitability for comparing two related samples without assuming a normal data distribution. Since normality could not be guaranteed, this approach offered a more robust analysis. The null hypothesis stated that there were no significant differences in pixel intensity values between the two techniques. Statistical significance was set at $p < 0.05$ for all analyses. Data organization and analysis were performed using SPSS software.

RESULTS

Threshold-based segmentation

The chosen threshold values for brain and lesion segmentation in each of the patient's most conspicuous lesion-containing slice are shown in Table 1. The patients are identified by a letter code in order to protect their anonymity. Numbers are used to identify the slices that were analysed.

To facilitate the presentation of results, only one slice's worth of visual findings will be shown at a time. All the figures are related to the subject S2, slice 2, for future reference.

The initial image for brain threshold-based segmentation, along with its outcomes, is shown in Figure 2. The threshold-based segmentation performed for the brain and its intensity map are displayed in Figure 3. The outcome of the segmented lesion is displayed in Figure 4. The segmented lesion and associated intensity map are displayed in Figure 5.

Semi-automatic segmentation

Just as the Threshold-based segmentation results section, only the same cut of the same sequence (subject S2, slice 2) will be displayed in the visual results.

The initial image for brain semi-automatic segmentation, together with its outcomes, is shown in Figure 6. The brain's intensity map and semi-automated segmentation are displayed in Figure 7. The outcome of the semi-automatically segmented lesion is displayed in Figure 8. The lesion's intensity map and semi-automated segmentation are displayed in Figure 9.

3D reconstruction

To obtain the 3D reconstruction of the patient to whom section 2 belongs (visual results presented in the previous sections), the ImageJ programme was used. The result is shown in Figure 10.

Statistics

Pixel intensity values were compared between two methods using the Wilcoxon signed-rank test. The analysis yielded a $Z=-1.690$ and a $p\text{-value}=0.091$, indicating a tendency for the threshold-based method to produce lower intensity values than the semi-automatic method. Despite this trend, the difference was not statistically significant ($p > 0.05$), suggesting that both methods can be considered equivalent in terms of pixel intensity at the 95% confidence level.

DISCUSSION

Threshold-based segmentation vs semi-automatic segmentation

Both segmentation methods have very similar threshold values. Visually, the results obtained through semi-automatic segmentation appear to be more accurate than the results obtained through Threshold-based segmentation. As we can see from Figures 2 and 6, the image obtained through Threshold-based segmentation shows a larger region of the skull, which is undesirable. In addition, the image obtained by Threshold-based segmentation shows larger gaps in the ROI in the image, which causes loss of necessary information. Regarding lesion segmentation, the visual results do not appear to be significantly different.

Both methods are prone to errors. In the case of Threshold-based segmentation, there is the inherent subjectivity of the human, and the contouring of anatomical components can be subjective even within the same subject¹⁵. In the case of automatic segmentation, the fact that the 2x ratio found between the threshold values was used to calculate the threshold value for segmenting the lesion can lead to two main errors: 1) the use of a factor approximated to unity instead of a value with more significant figures, and 2) the fact that the ratio has been found in a very limited database with no scientific support. This intensity-based segmentation is also affected by intensity inhomogeneity, noise, and partial volume, as well as overlap in intensities of brain and nonbrain tissue¹⁶. In addition, there may be errors due to the loss of information when converting images from DICOM to PNG¹⁷.

The result shows that there is no statistically significant difference between the segmentation values for both the threshold-based and semi-automatic methods. This means that this study does not invalidate the semi-automatic method proposed

but more research is needed to demonstrate that it is reliable method for brain and lesion segmentation.

It is proposed that any changes between the two procedures may also be clinically negligible because there is no statistically significant difference between them. This makes semi-automated segmentation a preferable alternative because it takes less time¹⁸.

3D reconstruction

Firstly, in both plans presented, there is an apparent loss of information in some areas of the brain. Analysing the slices one by one, we can in fact see that in a large part of the slices the segmentation has caused excessive loss of information. This is because all the cuts in the series were subjected to the threshold that was indicated for the slice with the most noticeable lesion. Secondly, both the cuts and the reconstruction show artefacts outside the region of interest.

Finally, and most obviously, in Figure 10 b) the 3D reconstruction is of poor quality, with a "staircase" appearance. 3D images are made up of voxels, pixels coupled with the thickness of the image slice. This is because the voxels are not isotropic, i.e., the depth of the slice has a different dimension to the width and height of the pixel.¹⁹Besides the use of a 2D sequence is more prone to errors than the common use of a 3D volumetric sequence.

Future directions

More research is needed to develop an accurate algorithm for brain and lesion segmentation, capable of doing this process not only in a faster way but that also surpasses the errors of the human eye and hand.

Some future work could include:

- The improvement of the *Matlab* code for automatic segmentation, to reduce artefacts and the loss of relevant information. This

involves applying the method to DICOM images, calculating a more appropriate threshold value for each slice of each sequence, and optimising the calculations performed by the code.

- Measuring and comparing the values obtained for the area and volume of the different brains and lesions, for the different methods.
- To study the potential quantifiable relationship between the threshold values for the segmentation of the brain and lesions.
- Increase the quality of 3D reconstruction using improved segmentation and another software, the *3D Slicer* programme.

FINAL CONSIDERATIONS

There are notable differences between paediatric and adult multiple sclerosis (MS) in terms of brain structure, lesion distribution, and disease progression. While most segmentation methods have been developed for adults, paediatric MS may require adapted approaches to address these unique characteristics. Our results suggest that the semi-automatic segmentation method has the potential to offer more accurate results in paediatric cases compared to threshold-based techniques. However, further research is needed to confirm these findings and develop more refined algorithms that effectively address the specific challenges presented by younger patients. Comparing Threshold-based segmentation and semi-automatic segmentation, results showed that the semi-automatic approach provided more accurate results, with a more accurate segmentation of the brain and less loss of information.

However, both methods presented challenges and possible sources of error. Threshold-based segmentation is prone to the subjectivity of the observer, while semi-automatic segmentation can be influenced by more specific factors, such as the choice of a verified relationship between threshold

values for lesion segmentation. In addition, the conversion of images from DICOM to PNG format may introduce some loss or alteration of information that could negatively affect the results.

The 3D reconstruction of the segmented images revealed some limitations, such as loss of information in certain areas of the brain and artefacts outside the ROI. A quality of the reconstruction was also affected by the non-isotropic nature of the voxels.

ACKNOWLEDGMENTS

We thank the Institute of Biomedical Engineering and Biophysics of the Faculty of Sciences of the University of Lisbon for its help in finding an internship to develop this project.

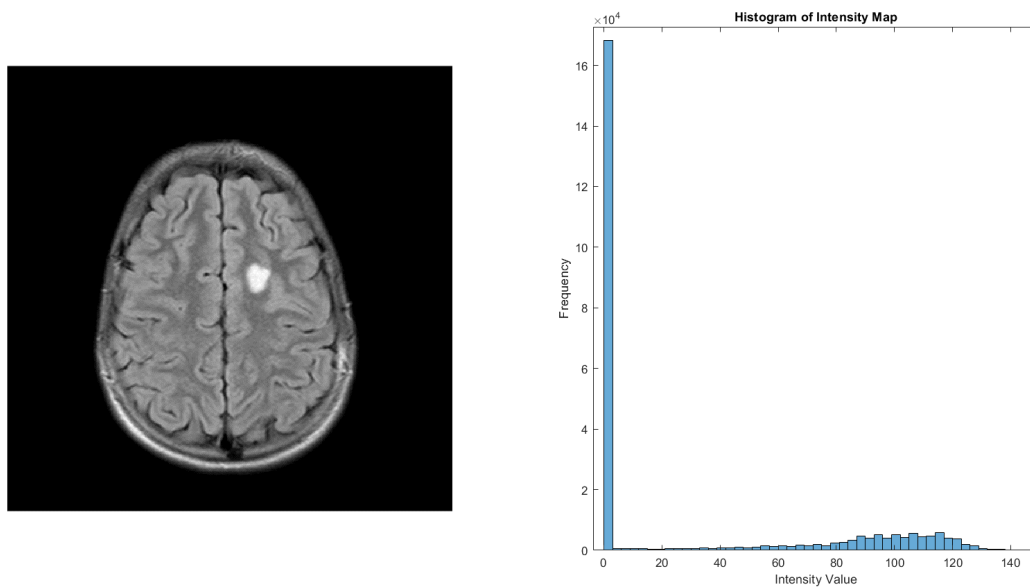
REFERENCES

1. Carvalho S, Pinto J, Correia I, Faustino R, Vasconcelos M, Sousa L, Palavra F. Inflammatory activity and treatment response in pediatric compared to adult multiple sclerosis: a pilot, retrospective and observational study of the first year after diagnosis. *Acta Med Port.* 2021;34(1):28-34.
2. Palavra F, Silva D, Fernandes C, et al. Clinical predictors of NEDA-3 one year after diagnosis of pediatric multiple sclerosis: an exploratory single-center study. *Front Neurosci.* 2023;17:1259306.
3. National Institute of Neurological Disorders and Stroke [NINDS]. Multiple Sclerosis. 2023. [citada 2023 junho 6]. Disponível em: <https://www.ninds.nih.gov/health-information/disorders/multiple-sclerosis>
4. Koch-Henriksen N, Thygesen LC, Stenager E, Laursen B, Magyari M. Patterns and predictors of multiple sclerosis phenotype transition. *Brain Commun.* 2023;6(6):fcae422.
5. Serviço Nacional de Saúde [SNS]. Dia Da Pessoa Com Esclerose Múltipla. 2023. [citada 2023 junho 5]. Disponível em: <https://www.sns.gov.pt/noticias/2020/12/04/dia-nacional-da-pessoa-com-esclerose-multipla/>
6. Hemond CC, Bakshi R. Magnetic resonance imaging in multiple sclerosis. *cold spring harbor perspectives in medicine.* 2018;8(5):a028969.
7. McDonald I, Compston A, Edan G, et al. Recommended diagnostic criteria for multiple sclerosis: Guidelines from the International Panel on the Diagnosis of Multiple Sclerosis. *Ann Neurol.* 2001;50(1):121-7.
8. Sinnecker T, Kuchling J, Dusek P, et al. Ultrahigh field MRI in clinical neuroimmunology: a potential contribution to improved diagnostics and personalised disease management. *EPMA J.* 2015;6(1):16.
9. Bakshi R, Ariyaratana S, Benedict RHB, Jacobs L. Fluid-attenuated inversion recovery magnetic resonance imaging detects cortical and juxtacortical multiple sclerosis lesions. *Arch Neurol.* 2001;58(5):742-8.
10. Trip SA, Miller DH. Imaging in multiple sclerosis. *J Neurol Neurosurg Psychiatry.* 2005;76 Suppl 3(Suppl 3):iii11-iii18.
11. Polman CH, Reingold SC, Banwell B, et al. Diagnostic criteria for multiple sclerosis: 2010 Revisions to the McDonald criteria. *Ann Neurol.* 2011;69(2):292-302.
12. Zeng C, Gu L, Liu Z, Zhao S. Review of deep learning approaches for the segmentation of multiple sclerosis lesions on brain MRI. *Front Neuroinform.* 2020;14:610967.
13. Radü EW, Sahraian MA, eds. *MRI Atlas of MS Lesions.* Springer Berlin Heidelberg; 2008.
14. Mortazavi D, Kouzani AZ, Soltanian-Zadeh H. Segmentation of multiple sclerosis lesions in MR images: a review. *Neuroradiology.* 2012;54(4):299-320.
15. Collier DC, Burnett SS, Amin M, et al. Assessment of consistency in contouring of normal-tissue anatomic structures. *J Appl Clin Med Phys.* 2003;4(1):17-24.
16. Despotović I, Goossens B, Philips W. MRI segmentation of the human brain: challenges, methods, and applications. *Comput Math Methods Med.* 2015;2015:450341.
17. de Bruijne M. Machine learning approaches in medical image analysis: From detection to diagnosis. *Med Image Anal.* 2016;33:94-97.
18. McGrath H, Li P, Dorent R, et al. Manual segmentation versus semi-automated segmentation for quantifying vestibular schwannoma volume on MRI. *Int J Comput Assist Radiol Surg.* 2020;15(9):1445-1455.
19. Crest + Oral-B dental care. Cone-Beam Computed Tomography (CBCT) Applications in Dentistry. 2023. [citada 2023 junho 10]. Disponível em: <https://www.dentalcare.com/en-us/ce-courses/ce531/voxel>

Table 1 – Threshold values selected both manually and by *Matlab* for brain and lesions segmentation and ratio between values selected manually

Subject	Slice	Threshold for Manual Brain Segmentation (TMC)	Threshold for Semi-Automatic Brain Segmentation (TSAC)	Threshold for Manual Lesion Segmentation (T _{ML})	Threshold for Semi-Automatic Lesion Segmentation (T _{SAL})	Ratio (T _{ML}) / (T _{MC})
S1	1	365	317.238	650	634.475	1.781
S2	2	80	73.5	140	147	1.750
	3	80	71.133	140	142.226	1.750
S3	4	310	303.544	600	607.087	1.935
S4	5	280	248.965	490	497.300	1.750
S5	6	60	71.135	140	142.269	2.333
S6	7	370	348.299	650	696.597	1.757
					Mean Ratio (SD)	1.865 ± 1.9 (0.267)

Figure 1 – Brain MRI from a MS paediatric patient



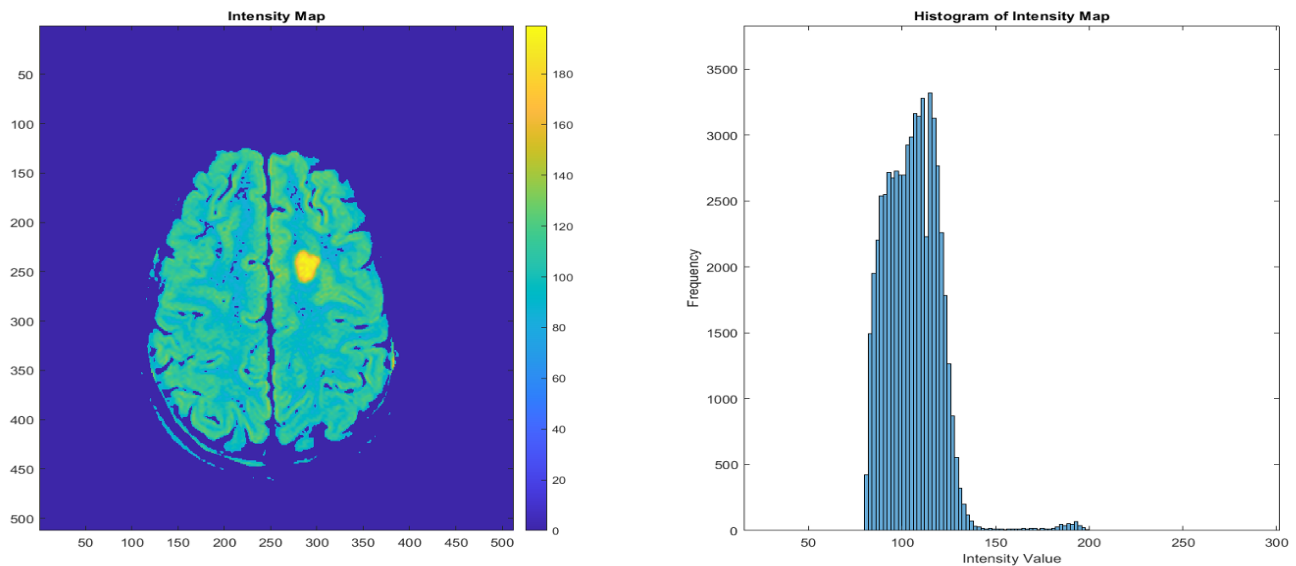
Original image of slice 2 from a T2-weighted FLAIR sequence of a MS paediatric patient (subject S2) (left H); Histogram of Intensity Map for the original image (right).

Figure 2 – Brain threshold-based segmentation



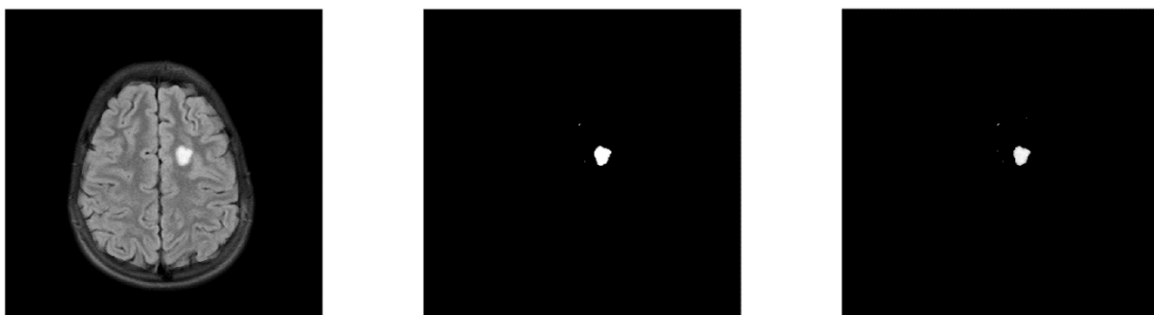
Original image of slice 2 from a T2-weighted FLAIR sequence of a MS paediatric patient (subject S2) with a 0.1 attenuation factor outside of the ROI (left); Mask created through threshold application for threshold-based segmentation (centre); Attenuated image with mask (right).

Figure 3 – Intensity map in brain segmentation



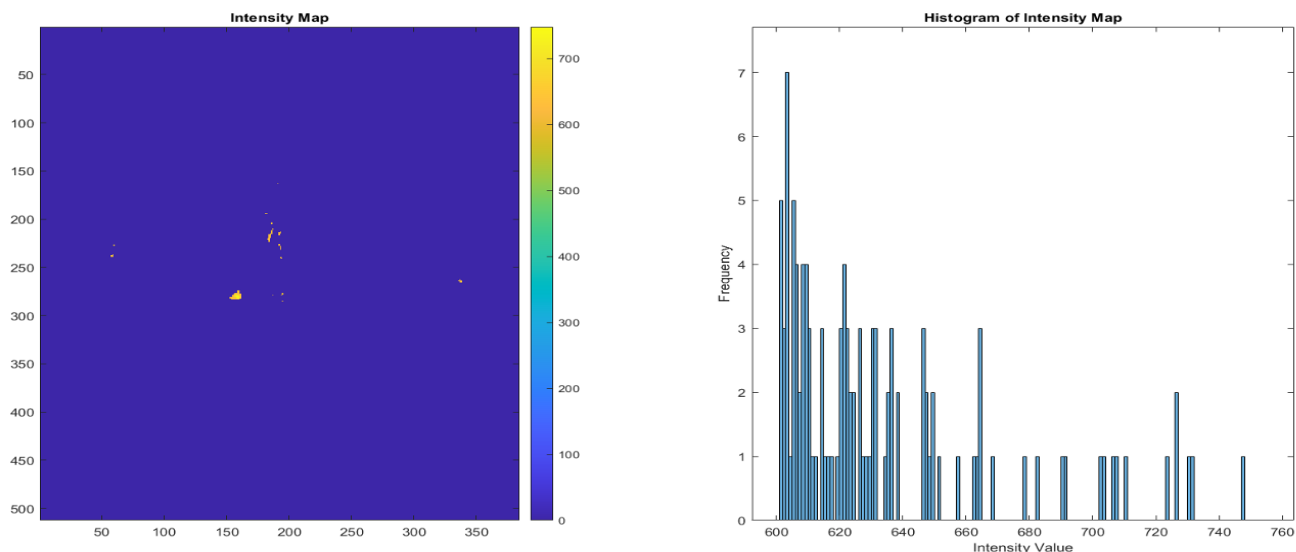
Intensity map for the segmented brain image (left); Histogram of the intensity map for the segmented brain image (right).

Figure 4 – Threshold-based segmentation of lesion



Original image of slice 2 from a T2-weighted FLAIR sequence of a MS paediatric patient (subject S2) with a 0.1 attenuation factor outside of the ROI (left); Mask created through threshold application for threshold-based segmentation (centre); Attenuated image with mask (right).

Figure 5 – Intensity map in brain lesion



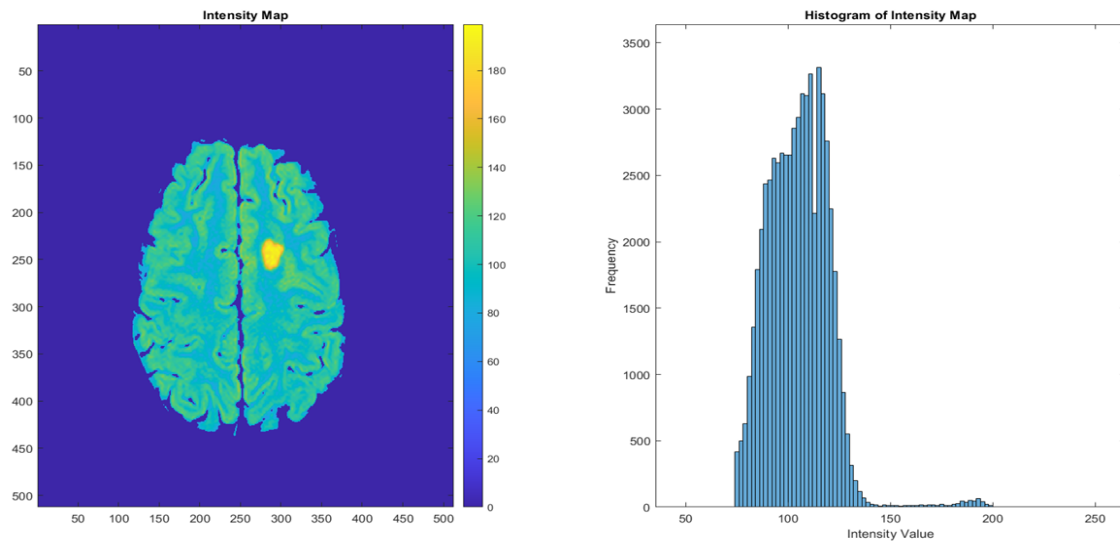
Intensity map for the segmented lesion image (left); Histogram of the intensity map for the segmented lesion image (right).

Figure 6 – Brain semi-automatic segmentation



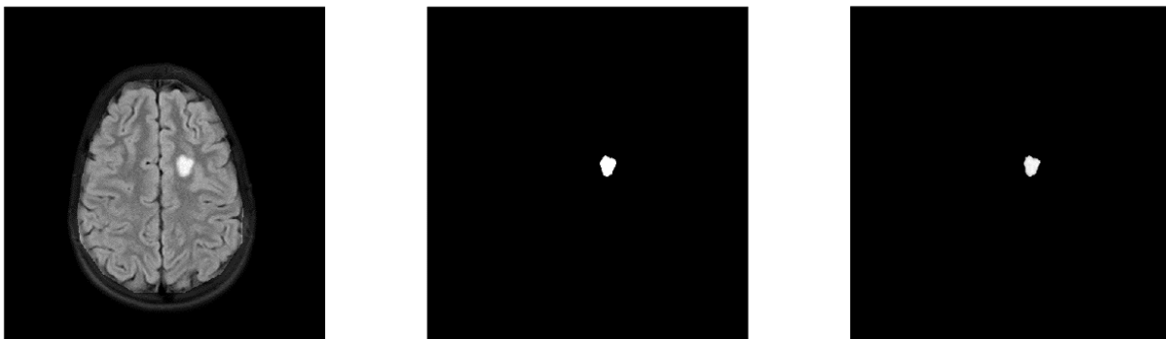
Original image of slice 2, from subject S2 with a 0.1 attenuation factor outside of the ROI (left); Mask created through threshold application for threshold-based segmentation (centre); Attenuated image with mask (right).

Figure 7 – Intensity map in brain segmentation



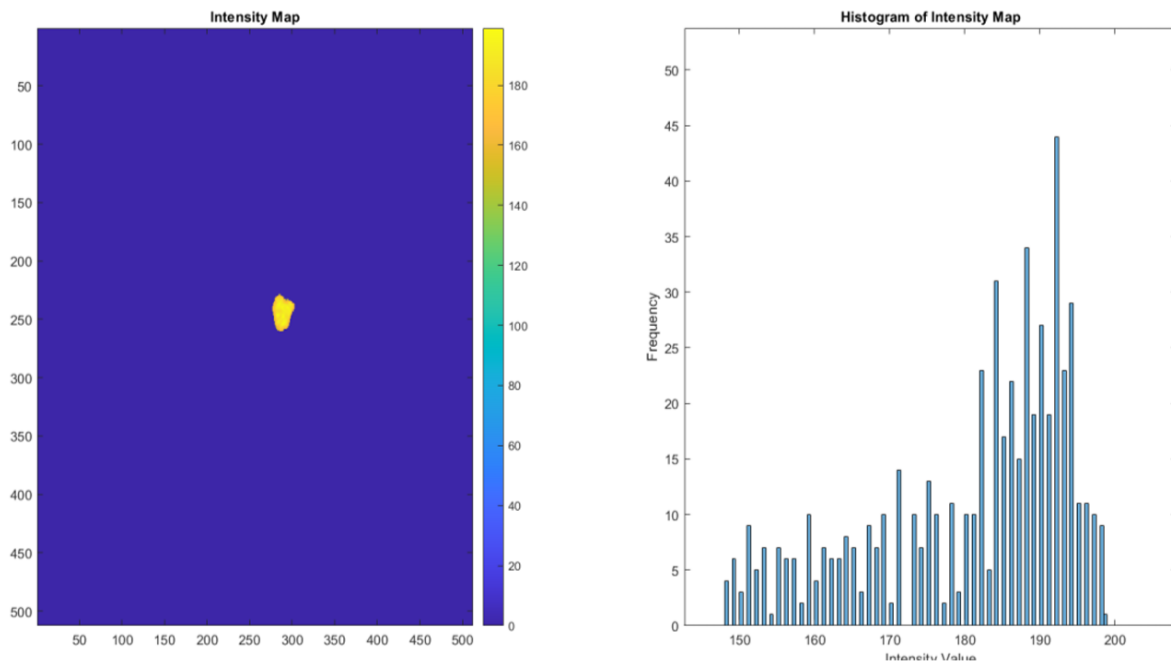
Intensity map for the segmented brain image (left); Histogram of the intensity map for the segmented brain image (right).

Figure 8 – Lesion semi-automatic segmentation



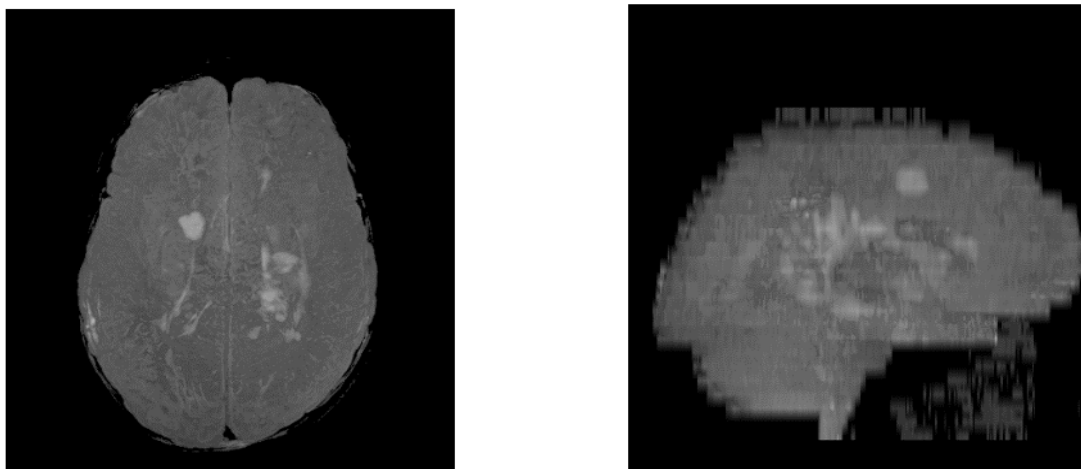
Original image of slice 2 from a T2-weighted FLAIR sequence of a MS paediatric patient (subject S2) with a 0.1 attenuation factor outside of the ROI (left); Mask created through threshold application for Threshold-based segmentation (centre); Attenuated image with mask (right).

Figure 9 – Intensity map in brain lesion



Intensity map for the segmented lesion image (left); Histogram of the intensity map for the segmented lesion image (right).

Figure 10 – 3D segmented brain reconstruction



Superior axial plane view from slice 2 from a T2-weighted FLAIR sequence of a MS paediatric patient (subject S2) (left); 3D reconstruction from a T2-weighted FLAIR sequence of a MS paediatric patient (subject S2) (right).